Hybrid propulsion control with enhanced lever haptics

C. de Keijzer, MSc *(§)*

R. Wagenaar, BASc *(§)*

E. Koppen, MSc *(§)*

§ Kwant Controls, Sneek

Synopsis

During the last decade, hybrid propulsion is proven as an upcoming method to save fuel onboard of vessels. Especially parallel drives with a diesel-engine and an electric machine with a DC electric network under power management system (PMS) control is of interest. Although fuel saving and emission reductions of seagoing vessels are achieved, the safety of manoeuvring must remain priority. Under all circumstances the master must be certain that the demanded thrusts are achieved from the selected station-in-control. For hybrid propulsion so far, much emphasis has been put on PMS from rule-based, via linear programming to grey wolf methods. However, the impact of the human factors on safety of manoeuvring the vessel has not yet attracted much interest. In most cases various modes of operation are selectable via touch-screens.

This paper introduces a method for power management and propulsion mode selection by the use of the propulsion levers with haptic feedback. Instead of touch-screens, the levers, in conjunction with the measured speed-through-water and other variables, are used to estimate the required propulsion load. An advanced rule-based PMS system is used to set the required generator loads and to control the charging and discharging of the batteries. The PMS system uses the lever-based power estimation. Via force feedback and vibration of the lever-in-control, the master is informed about the machinery state and starting / stopping sequences. The lever-in-control can be at various stations. All devices, including rudders and other manoeuvring enhancing devices are under a single control transfer regime.

Furthermore, this paper describes and analyses the safety benefits of intuitive control inputs and machinery state feedback on base of tactile feedback. For the transit mode it is shown, that more fuel-saving is possible by using the power / reversing levers for the load prediction, compared to only using PMS with conventional mode selection. In harbour mode the emphasis is on achieving the required thrusts and yaw moments as fast as possible and in the most efficient way.

Keywords :

Lever haptics, intuitive propulsion control, battery hybrid, fuel efficiency, power reversing lever, lever controlled mode transition

Author's biographies

Coen de Keijzer graduated in 2013 at the Rotterdam School of Management Erasmus University where he obtained a BSc in Business Administration. In 2015 he obtained his MSc degree in Business Information Management. Currently he is responsible for the sales and marketing of Kwant Controls.

Ronny Wagenaar graduated in 2003 at the NHL Stenden Hogeschool. He has obtained a BASc in Electric Engineering. Currently he is Lead Systems Engineer at Kwant Controls.

Emil Koppen graduated in 2009 at the University of applied science where he obtained a BASc (including AVL Schrick honor). In 2010 at the Technical University of Eindhoven, he obtained his BSc and in 2013 his MSc (with great appreciation) in Automotive Technology. Currently he is responsible for the Research and Development of Kwant Controls

1. Introduction

For many decades the Power Take-In (PTI) electric motor has been coupled to the propeller-shaft of single screw vessels, to take over the single diesel-engine for homecoming. The power take-off (PTO) generator in conjunction with a controllable pitch propeller (CPP) is also well-known for vessels requiring power to drive for example transverse thrusters. The alternating current (AC) electric network requires the PTO shaft-generator to be driven at constant speed.

The traditional power reversing lever (PRL) is used together with a combinator to generate the pitch and shaft-speed demands for various modes of operation (Figure 1). The lever is equipped with simple haptic feedback: one detent at the zero thrust position.
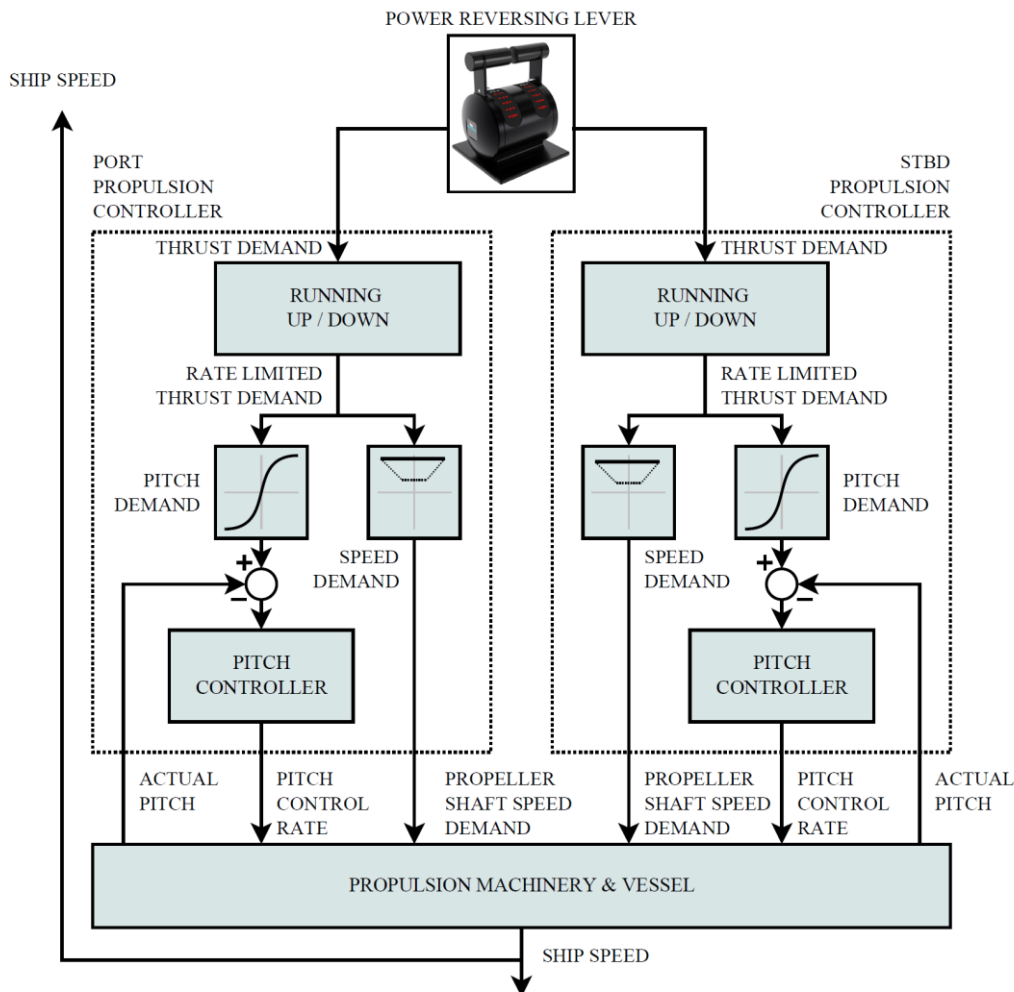
Figure 1: Basic propulsion control by propeller pitch & shaft speed combinator

Developments in power electronics [Bossert et al. 2017], on the basis of a direct current (DC) electric network with frequency converters, allowed to apply shaft-generators with variable propeller-shaft speed. The development of battery technology made electrical energy storage also feasible for seagoing vessels. The necessity to save fuel, let to the emergence of battery-hybrid propulsion.

Hybrid propulsion allows for various propulsion modes, generally more complicated than the previous diesel-mechanical propulsion systems with PTO or PTI. As a consequence, the master has many degrees of freedom to select a propulsion mode in order to safely manoeuvre and save fuel. Complexity requires automation to limit the master's workload and support with awareness of abnormalities including the required mitigations. A task such as propulsion mode transition by engaging / disengaging driving machines requires many actions. For example speed synchronization and load shedding. Modes are controlled via touchscreens, during mode transitions the master has to watch the progress of the mode transition at displays which limits the masters' attention (see Figure 2). This paper presents a method to improve safety by embedding bi-directional interaction with the master about the hybrid propulsion system via haptic devices.

A certain propeller thrust is required for safe manoeuvring. Based on the observed vessel motions, the experienced master intuitively knows which amount of thrust is needed. The PMS calculates the required power which determines the optimum and safe propulsion mode as well as commands the respective machines to engage / disengage. During this process of transition, the master receives kinaesthetic force and vibro-tactile feedback via the lever regarding the machinery states.
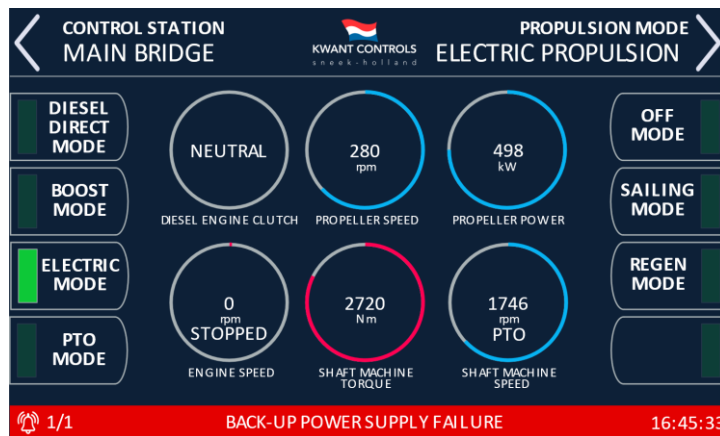
Figure 2: Example touch-screen display for mode selection of a hybrid propulsion system

The recent accident with the USN destroyer John McCain [National Transportation Safety Board 2017] gives, besides other aspects like tiredness, an example on over-automation. Also in the aerospace industry crew awareness is improved, by the use of active side-sticks [Rauer 2019]. The lever haptics presented in this paper result in more safety during manoeuvring by simplification and an intuitive user interface.

1.1. Hybrid propulsion

Although electric shaft-machines as PTO-generators or PTI-motors exist since many decades, the addition of batteries for energy storage resulted in various onboard battery-hybrid solutions, such as:

- Emission reduction by power peak shaving for harbour tugs, anchor handling tugs, etc.
- Availability of boost power for high-speed runs of naval crafts and yachts
- Fuel savings on workboats like trailing suction hopper dredgers or fishing vessels
- Emission free manoeuvring of ferries in urban areas

This actual hybrid system configuration strongly depends on the mission profile of the vessel [Bossert et al. 2017, Grimmelius et al. 2011, Einsiedler 2017]. A trailing suction hopper dredger requires a different configuration as a harbour tug or ferry. In this paper, a hybrid RoPax ferry propulsion system with many degrees of freedom for setting thrust levels (as depicted in figure 3), will form the example to illustrate the lever haptics.
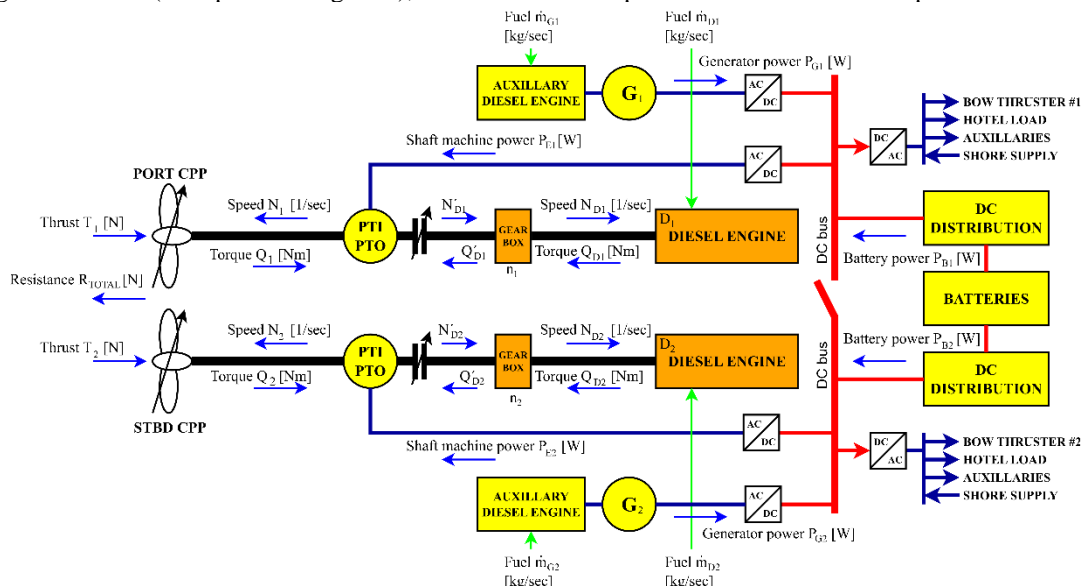
Figure 3: Hybrid propulsion system for a ferry with a controllable pitch propeller

The classical RoPax ferry is propelled by a port side (PORT) and starboard side (STBD) CPP, each driven by twin diesel-engines. A PTO-generator, running at a constant speed, is added to each shaft-line to provide sufficient power during the harbour mode for the transverse thrusters. For the hybrid ferry, instead of two diesel-engines, one diesel-engine and one shaft machine can be used. Figure 3 depicts a slow-speed direct drive shaft-machine, which can act as PTI motor and as PTO-generator. For RoPax ferries, batteries are needed for emission free manoeuvring in harbour areas and while berthing / unberthing under calm wind conditions by using the PTI motor.
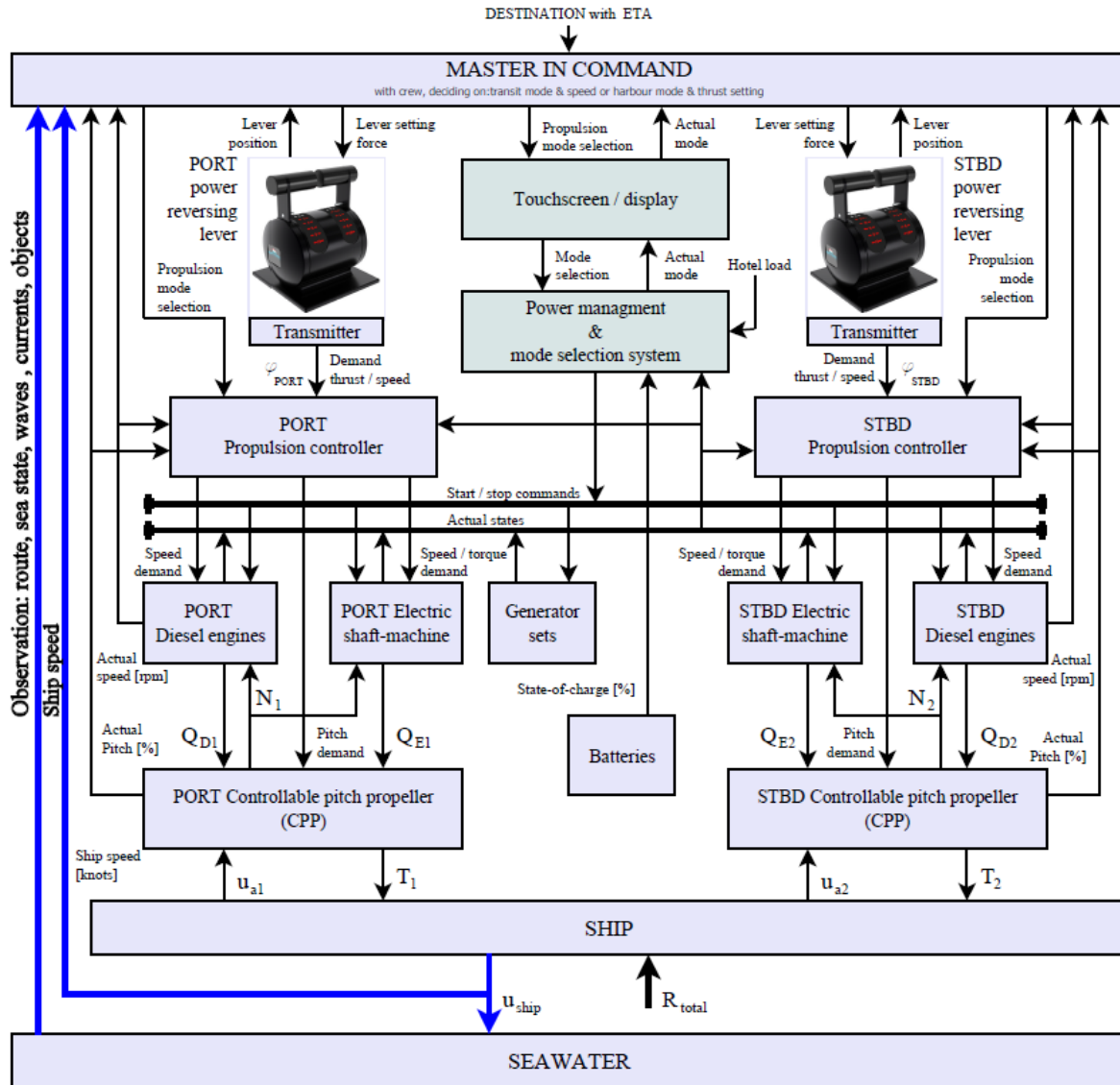
Figure 4: Overview of hybrid propulsion control

In Figure 4, for remote control of these various propulsion modes (even more with the additional energy sources), normally a touch-screen / display is integrated. This increases the burden of the master and distracts him from making external observations of obstacles and unsafe situations. Watching the display is not always possible, since attention is required for external observation.

2. Lever haptics

2.1. General

Human haptics refers to the human sense of touch and movement. Within the field of haptics, one of the most important subjects, besides the neuromuscular system and the cognition process, is human perception. A haptic device is a mechanical device designed to provide (kinaesthetic) force and vibro-tactile feedback, coupled to an indirect interaction with a real and/or virtual environment [Qin et al. 2015, Barrow and Harwin 2016, Gosselin et al. 2016]. Kinaesthetic feedback haptics deals with devices that interact with muscles and tendons which gives humans the sensation of force being applied. Vibro-tactile feedback deals with the devices that interact with the nerve endings in the skin which indicates heat, pressure and texture. Applications using haptic kinaesthetic and vibro-tactile interfaces, for example in robotics and computer technology, are well known for years [El Saddik et al. 2012, Haruhisa 2015, Pacchierotti 2016, Van der Linde et al. 2002]. Still much more research is required to define application specific requirements for the mechanisms and controls in terms of magnitudes and bandwidths that compose human haptic perception [Colgate and Brown 1994, Boff and Kaufman 1986, Rovers et al. 2003]. Sensing bandwidth refers to the frequencies with which kinaesthetic and/or vibro-tactile stimuli are sensed. Control bandwidth refers to the frequencies at which humans can respond and voluntarily initiate motion of their limbs. The human input (sensory) bandwidth is much larger than the output bandwidth and the human response to physical indication is much faster compared to visual observation. Additionally, it is critical to ensure that the level of haptic feedback is sufficient for task completion while being comfortable for the operator. The capabilities of the human sensory system are important for successful haptic control design. Literature based and application related conclusions are summarized below [Kilchenman and Goldfarb 2001, Shimoga 1992].

- Kinaesthetic sensing bandwidth of 20 to 30 [Hz]
- Vibro-tactile sensing has a bandwidth of 0 to 400 [Hz]
- Fingers and hands have a force exertion bandwidth of 5 to 10 [Hz], for Limbs $2 - 5$ [Hz]. A single finger can retain a force of up to 7 [N] without experiencing discomfort or fatigue, while hands can retain force levels of 30 to 50 [N]
- Experiments show that the performance of test-persons did not improve when the haptic control device was using frequencies with a bandwidth > 40 [Hz] and an endpoint force level > 3 [N]

Remote control (via x-by-wire technology) enables flexible engineering of relationships between control input and the controlled element. They allow amplification of forces, filtering, system limitations, but remove the bi-directional haptic kinaesthetic and vibro-tactile interaction. Therefore the haptic bi-directional operator interaction is getting even more beneficial for complex control structures.

2.2. Types of lever haptics

The critical component of a haptic device is its mechanism, which defines the motion capabilities of the human operator when interacting. Sensors track the operators' lever motion and the actuators deliver the desired forces or textures to the operator (as shown in Figure 5).
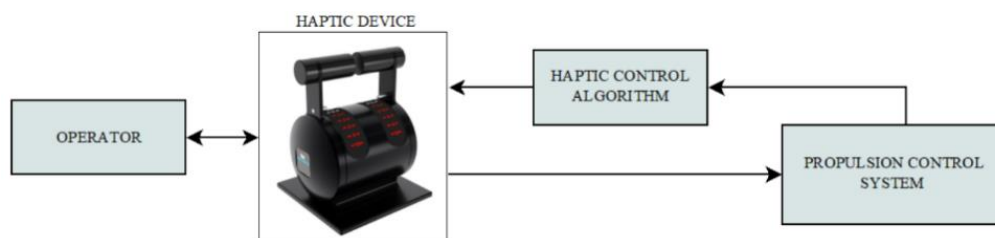
Figure 5: Overview of haptic device integrated into a propulsion control system

The operator (master in control at the bridge), for the design of a haptic device, a model of the operators' arm and hand are of high importance. The exact modelling of a human arm remains a complex problem [Grunwald 2008], many approaches are available in literature, mainly for passive responses [Kosuge et al. 1992, Lawrence 1993, Tsuji et al. 1994]. Several dynamic models are available, however most of the parameters are uncertain and have a large range that also depend on the person itself. The dynamics are even more complicated, when the human/operator is coupled to the haptic device. Subjects as structural flexibility, grapping conditions and reflex delays must be considered.

The haptic device, in this hybrid propulsion use-case called the PRL, is a mechanical interface operated by the operator mainly for controlling the power and its' direction of the operated vessel. Figure 6 shows the basic setup of the PRL, whereas the (approximated) general equation of motion is given in (1). The precise position and especially velocity measurement is required for high performance haptic applications [Ghaffari and Kövecses 2013, Chawda et al. 2018]. Adjustable and optimized mechanical friction is required for safety purposes. PRLs are designed for strength and stability, operated with the palm and fingers. The actuator bandwidth is up to 50 [Hz] in order to meet the dynamic requirements.
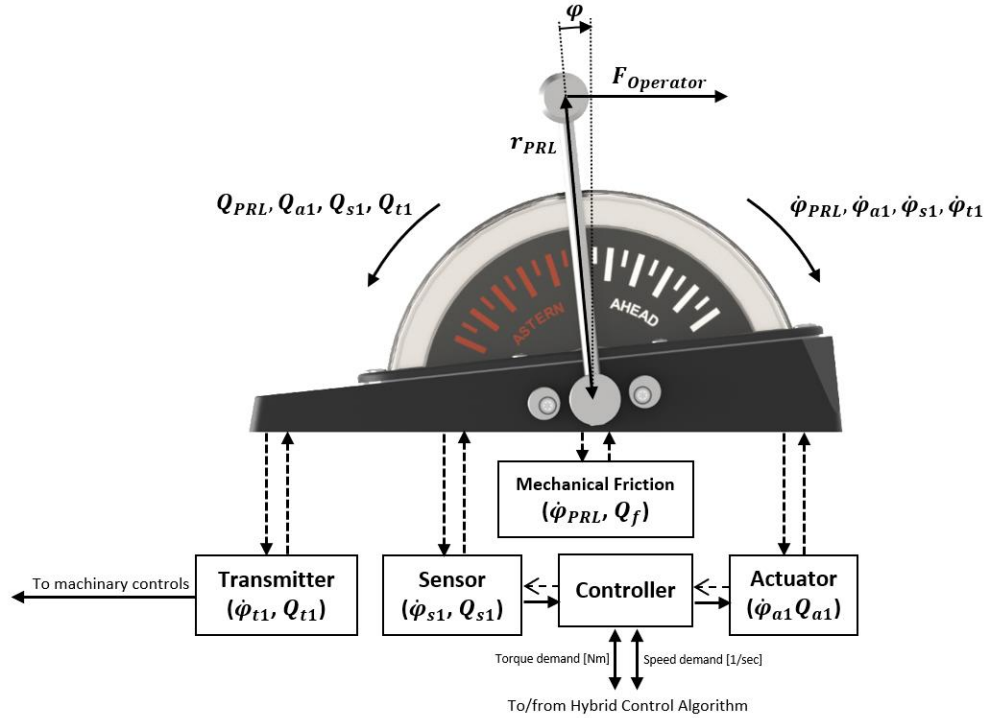
Figure 6: Schematic overview of haptic device

The (approximated) general equation of motion:

$$\sum Q = \sum J\,\ddot{\varphi} + \sum D\,\dot{\varphi} + M\,\sin(\varphi) \tag{1}$$

where:

$$\sum Q = Q_{PRL} - Q_{operator} \tag{2}$$

$$Q_{PRL} = Q_{t1}z_{t1} + Q_{s1}z_{s1} + Q_{a1}z_{a1} + Q_F + Q_{gPRL} \tag{3}$$

$$\sum J = \left(J_{t1}z_{t1}^2 + J_{s1}z_{s1}^2 + J_{a1}z_{a1}^2 + J_{gPRL}\right) \tag{4}$$

$$\sum D = \left(D_f + \frac{D_{a1}}{z_{a1}^2}\right) \tag{5}$$

$$M = m_{PRL}\,g\,r_{PRL} \tag{6}$$

$$z_{t1} = \frac{\varphi_{t1}}{\varphi_{PRL}}; \; z_{s1} = \frac{\varphi_{s1}}{\varphi_{PRL}}; \; z_{a1} = \frac{\varphi_{a1}}{\varphi_{PRL}} \tag{7}$$

The haptic control algorithm, must be intuitive as well as robust against disturbances (including the operators' interaction) and uncertainties (including friction and inertia errors). Several types of haptic patterns are investigated; friction, spring force, detents, vibration and/or in combination with audio-visual assistance.

- (Dynamic) friction

Dry-friction is a complex phenomenon, arising as the force that resists the relative motion of (solid) surfaces sliding against each other. Much research has been performed, but still a lack of dynamic high realistic models remains [Karnopp 1985, Armstrong-Hélouvry et al. 1994, Bernstein et al. 2005]. Friction can be divided in static (dry) friction and dynamic (kinetic) viscous friction. The transition between static and dynamic can be characterized with the Stribeck friction [Ueberle 2006]. The Stribeck friction is a nonlinear low-velocity friction effect that dominates stick-slip motion. Dynamic friction is based on velocity, the resolution presents serious algorithms for high performance haptic devices [Chawda et al. 2018]. Friction is mechanically implemented in the PRL for safety reasons, additional dynamic friction will be added by the haptic control algorithm according to the following approximation (8).

$$Q_{a1} = \begin{cases} (Q_{Coulomb}\{\varphi\} + Q_{Stribeck}\{\varphi - \varphi_{Stribeck}\} + Q_{viscous}\{\dot\varphi\}) & \varphi < -\gamma\varphi \\ (Q_{Coulomb}\{\varphi\} + Q_{Stribeck}\{\varphi - \varphi_{Stribeck}\} + Q_{viscous}\{\dot\varphi\}) & \gamma\varphi < \varphi \end{cases} \tag{8}$$

Where γ is the near to zero velocity band, variations can be created in different friction viscous levels, characteristics and coarseness effects as shown in Figure 7.
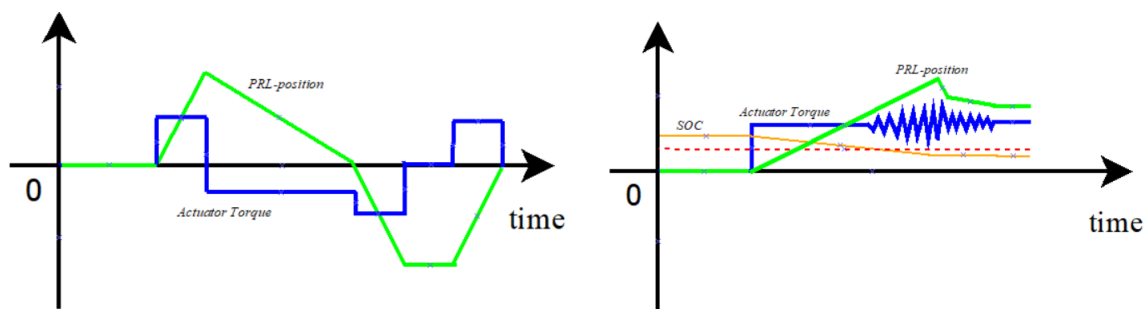
Figure 7: Examples of (dynamic) friction torque profiles as function of PRL-position

- Spring force

The kinaesthetic spring force feedback is a haptic pattern where the force is directly related to the position and movement direction. The force always points to the opposite direction of the motion, so working against the operators' movement. The spring effect and resulting return force functionality enables force orientation. The return force can be limited in order to avoid unwanted lever movements not initiated by the operator. Variations can be created in spring characteristics, symmetrical characteristics and force levels (see Figure 8). Special attention is required for the implementation in steering haptic devices. Noting that it can also be used for forbidden operating areas.
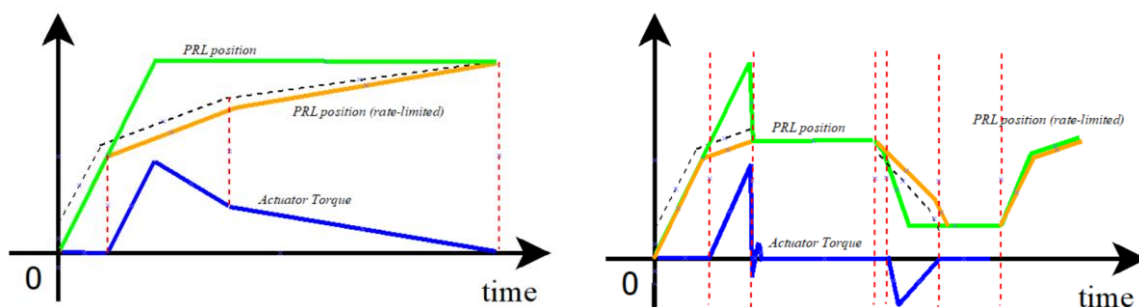
Figure 8: Examples of spring force torque profiles as function of PRL-position

- Detents/bumps/clicks

Detents/bumps/clicks are established for decades as fixed position feedback for the PRL, mostly for zero/neutral reference. This feedback gives no information about the controlled system and is therefore no haptic bi-directional interaction. Literature shows that surface and texture features can be represented by forces [Minsky 1995]. Different position feedback shapes are known from literature, controlling the force as function of position. The force shapes vary from hills to complicated holes. The position of the force shape, which is relatively small, forms an important characteristic. Further variation is found in the relative force-levels to distinguish between different PRL positions (see Figure 9).
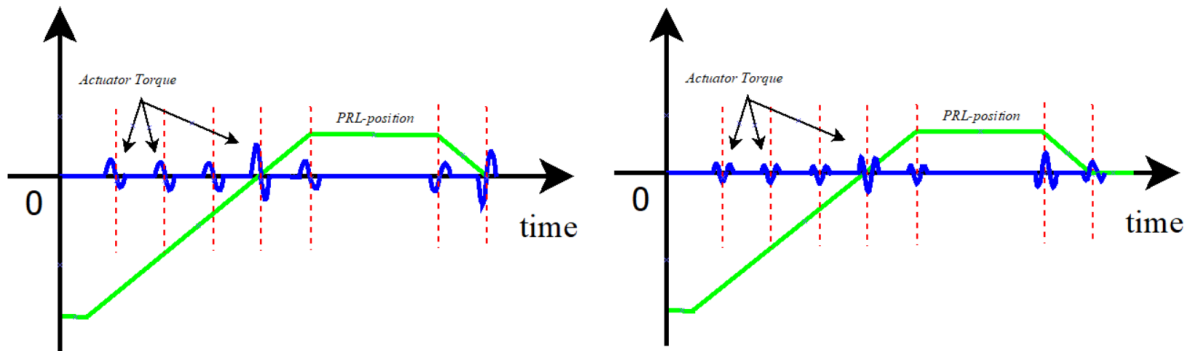
Figure 9: Examples of detent/bump/click torque profiles as function of PRL-position

- Vibro-tactile

Vibro-tactile feedback as guidance can be divided in attentional and movement/spatial guidance. The movement guidance is used to guide human movements in a precise way towards a specific target. In order to interfere with the operators' concentration and automatic reaction, the vibro-tactile guiding methods should be intuitive. The haptic vibro-tactile patterns and their meaning require learning [Weber et al. 2011]. Vibro-tactile feedback in haptic devices can be described in terms of intensity, rhythm and duration. The intensity can be considered as a parameter that can be affected in combination with both, rhythm (frequency, amplitude) and duration (time) as shown in Figure 10 [Asif et al. 2010].
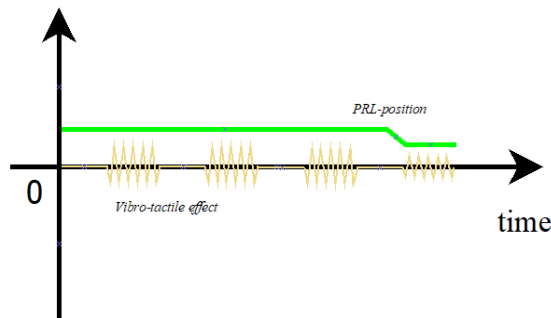
Figure 10: Examples of vibro-tactile profiles as function of PRL-position

3. Power management and lever haptics

The master is responsible to safely berth the ferry at the expected time of arrival (ETA). Typically two modes of operation exist:

- Harbour mode: manoeuvring at low speed close to and in the harbour and berthing at the quay. The required power for safe manoeuvring is mainly determined by actual wind conditions and tidal currents. The position of the lever is proportional to the actual propeller (bollard) thrust.
- Transit mode: sailing at a constant service speed such that the minimum amount of fuel is consumed. The power is mainly determined by the ships' resistances.

Figure 11 shows the hybrid propulsion system of figure 3 with the addition of lever haptics. The master selects the mode of operation (harbour or transit mode) and uses the PRL to set the required propulsion thrust or vessel speed. The required power is estimated by the haptic control algorithm. The machinery and power management module ensures that the required power is available by starting and stopping the required machinery. The available power is determined by the running and engaged motors or diesel-engines and their allowed maximum load level. The difference between actual required power and available power is used by the haptic control algorithm, that controls the haptic device of the PRL.
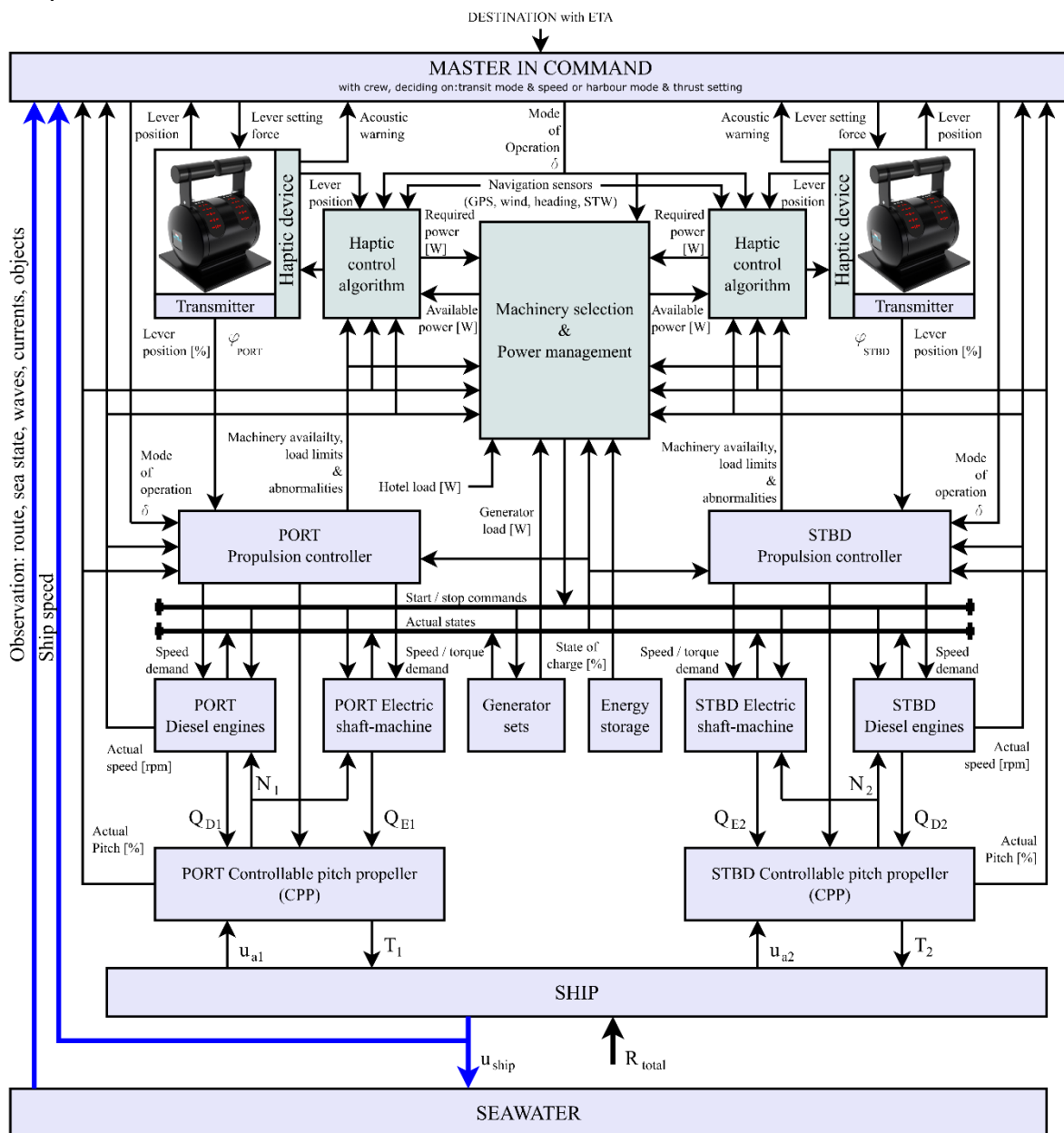
Figure 11: Overview Hybrid propulsion control with lever haptics

During transit mode, fuel efficiency has second highest priority, safety of manoeuvring remains first. The master knows how to set the vessel speed for the various legs of the selected voyage. The set PRL demand (vessel speed) is verified by checking the ships' motions. During transit mode, the PRL is only touched to change the vessels' speed. For any abnormality, such as slow-downs, the lever position is accordingly adjusted by the haptic device and the masters' attention is drawn by visual and acoustic warnings.

The ferry operations for a one way voyage are shown in Table 1. During (un)loading, the vessels' batteries are charged using energy from the shore connection and/or the on-board auxiliary generators. For unberthing the vessels' main clutches are engaged, batteries are near to full and the vessel can be unberthed and manoeuvred in harbour mode. Using the shaft machines as propulsion motors (reducing the batteries' SOC) assisted by both diesel engines, if wind conditions require. When the vessel is at open sea, the master selects transit mode. The charging of the batteries can efficiently be done by using the PTO generators assisted by auxiliary generators, depending on the requested service speed / power request (sailing part 1). When the batteries are near to full (not full to allow energy storage during a crash-stop), the propulsion mode is changed to enable fuel-efficient sailing (sailing part 2). For arrival, harbour mode is used (equal to the departure procedure only in reverse order).

No	Vessel operation	Fuel saving	Emission reduction	Thrust response	Charging / Discharging	Propulsion mode	Propulsion mode
1	Loading	-	++	-	Charging	Harbour	OFF, PTO
2	Unberthing	-	++	++	Discharging	Harbour	ELECTRIC, DIESEL DIRECT
3	Manoeuvring	-	++	++	Discharging	Harbour	ELECTRIC, DIESEL DIRECT
4	Sailing (part 1)	+	-	-	Charging	Transit	PTO assisted with genset when necessary
5	Sailing (part 2)	++	-	-	Discharging	Transit	ELECTRIC, DIESEL DIRECT, BOOST
6	Manoeuvring	-	++	++	Discharging	Harbour	ELECTRIC, DIESEL DIRECT
7	Berthing	-	++	++	Discharging	Harbour	ELECTRIC, DIESEL DIRECT
8	Unloading	-	++	-	Charging	Harbour	OFF, PTO

Table 1: Overview on vessel operations and key parameters

3.1. Haptic control algorithm

Figure 12 and Figure 13 show the haptic control algorithm, machinery selection and power management system of Figure 11 in more detail.
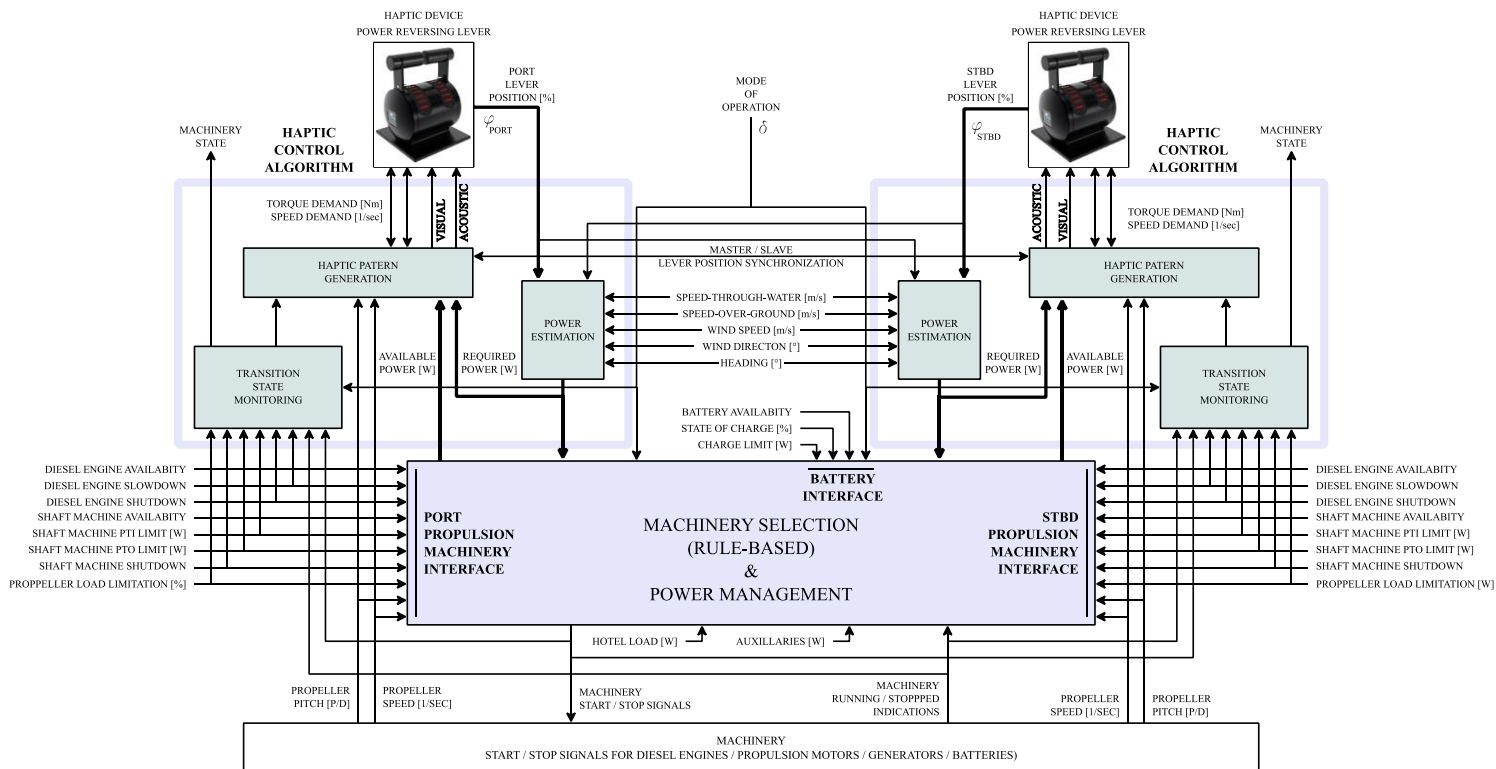
Figure 12: haptic feedback system for hybrid propulsion control

The haptic control algorithm exist of three sub modules:

1) Power estimation, to estimate the required propulsion power,
2) Transition state monitoring, monitoring of the status of ongoing propulsion mode transitions and actual machinery states,
3) Haptic pattern generation, generating kinaesthetic and vibrotactile force as well as acoustic and visual feedback in the PRL.

The most important interfaces are the levers' position, required and available power (thick lines). In order to cope with existing regulations, the machinery state is made available for various displays.
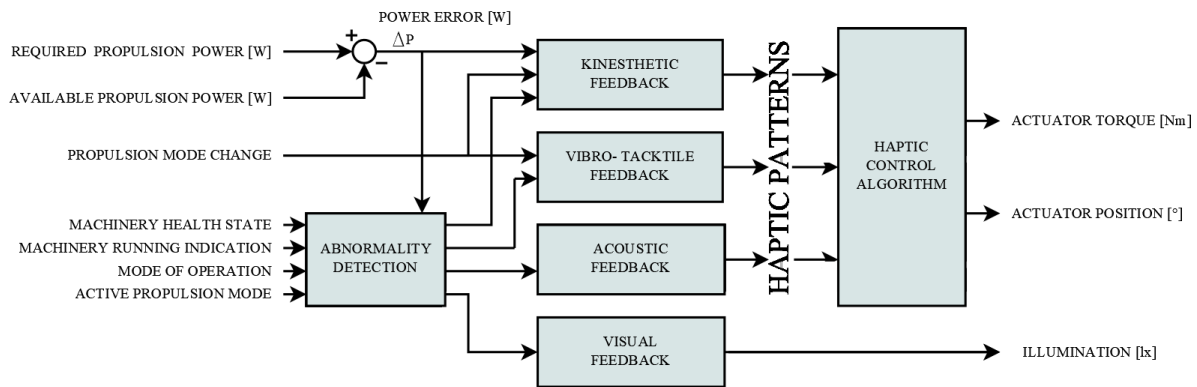
Figure 13 Overview of the hybrid pattern generation module

Figure 13 shows the different types of haptic feedbacks. The kinaesthetic feedback is based on ΔP, the difference between the required and available power. When ΔP becomes low, a kinaesthetic force as function of the ΔP is applied to inform the master that no additional power is available. The vibro-tactile, acoustic and visual feedback is used for abnormalities (warnings) and during propulsion mode selection.

3.2. Required power estimation

The estimation of the required propulsion power is based on the PRL demand set by the master and the mode of operation δ (transit or harbour mode). For harbour mode, u_{wind} with respect to the ship, mainly determines the power. For transit mode, the vessels' resistance (based on speed through the water u_{ship}) is mainly taken into account.

3.2.1. Power estimation in harbour mode of operation

The following equation (9) shows the approximate propeller thrust (T_n) as function of the propeller speed N_n and propeller pitch α_n (bollard condition), where C_t is the thrust coefficient and R the pitch force polynomial:

$$T_n \cong C_t \cdot N_n{}^2 \cdot \alpha_n{}^R \tag{9}$$

The thrust force to overcome the wind force is calculated by using [Blendermann, 1994]:

$$T_{x\_wind} = \frac{1}{2} \cdot \rho_{air} \cdot A_F \cdot CX_{AF}(\varepsilon) \cdot u_{wind}{}^2 \tag{10}$$

The required thrust for the low-speed harbour mode can be determined by the maximum of the longitudinal wind force and the lever thrust-demand, multiplied by a safety factor:

$$T_{n_{required}} = \max\left(\left|T_{x_{wind}}\right|, \left|\varphi_n \cdot T_{MAX}\right|\right) \cdot K_{safety} \tag{11}$$

The safety factor is a programmable factor based on amongst others:

- Vessels' location, manoeuvring in small ports or ports with high traffic and increased risk
- Water depth, influencing the thrust output of the propellers.
- Visibility, manoeuvring in dusk, dawn or dense fog increasing the safety factor.

$$K_{safety} = f_1(\delta, vessel_{location}, depth, visibility,) \tag{12}$$

Via the combinator diagram and (9) the required power for harbour mode can be determined:

$$Q_{n\_required} \cong |N_n| \cdot N_n \cdot (K_{cpp0} + K_{cpp} \cdot \alpha_n{}^P) \tag{13}$$

$$P_{n\_required} \cong 2\pi \cdot N_n \cdot Q_{n\_required} \tag{14}$$

During harbour manoeuvring also the transverse thrusters are used. The required thrust for the transverse thrusters can be determined as the maximum of the sideways wind force T_{y_wind} [Blendermann, 1994] and the bow thruster thrust-demand, multiplied by the safety factor:

$$T_{thrusters\_required} = \max(|T_{y\_wind}|, |\varphi_{thrusters} \cdot T_{thrusters\_max}|) \cdot K_{safety} \tag{15}$$

The required power for the bow thrusters is:

$$P_{thrusters} = \max(P_{thrusters\_max}, T_{thrusters\_required} \cdot K_{power}) \tag{16}$$

The final power requirement $P_{total\_required}$ is shown in equation 17:

$$P_{total\_required} = P_{1\_required} + P_{2\_required} + P_{thrusters}(u_{water}) + P_{hotel} + P_{aux} \tag{17}$$

3.2.2. Power estimation during transit mode of operation

During transit mode, the PRL gives the vessels' speed demand and the transverse thrusters are off. For transit mode, the power requirement depends on the vessels' resistance as shown in equation 18.

$$P_{total\_required} = f_2(R_{total}, u_{ship}(\varphi_{PORT}, \varphi_{STBD}), u_{wind}, waterdepth) \tag{18}$$

3.3. Available power

The available power (23) is the sum of the maximum diesel-engine power (19) and the electric shaft-machine power in PTI-mode (21) or in PTO-mode (22).

$$P_{Dn}(n_{Dn}) = \begin{cases} 0, & D_n \neq running \\ min(P_{Dn\_MCR}, P_{Dn\_SLOWDOWN}, P_{LOAD\_LIMIT}), & D_n = running \end{cases} \tag{19}$$

When the shaft machine is used as propulsion motor (PTI) the maximum available power for driving the propulsion motor P_{En_PTI} is the minimum of:
1) maximum allowed shaft machine power $P_{En\_PTI\_PWR\_LIMIT}$.
2) total available electrical power from the generators P_{Gn} and battery system P_{Bn} power minus the total hotel load P_{HOTEL} and maximum transverse thruster power reserve P_{MAX_THR} (harbour mode).

$$P_{En\_PTI\_PWR\_LIMIT} = \min\left(Q_{En\_MAX\_TORQUE}, \frac{P_{PTI\_MAX}}{2\pi \cdot N_{En}}\right) \tag{20}$$

$$P_{En\_PTI}(n_{En}) \begin{cases} 0, & E_n \neq running \wedge PTI \\ min\left(P_{En\_PTI\_PWR\_LIMIT}, (P_{Gn} + P_{Bn} - P_{HOTEL} - P_{thrusters})\right), & E_n = running \wedge PTI \end{cases} \tag{21}$$

When the shaft machine is used as generator (PTO) the maximum available electric power is the minimum of:
1) maximum allowed shaft machine power $P_{En\_PWR\_LIMIT}$.
2) total required electrical power for the hotel load P_{HOTEL} and maximum transverse thruster power $P_{thrusters\_max}$ (harbour mode).

$$P_{En\_PTO}(n_{En}) = \begin{cases} 0, & E_n \neq running \wedge PTO \\ min(P_{En\_PTO\_PWR\_LIMIT}, (P_{HOTEL} + P_{thrusters\_max})), & E_n = running \wedge PTO \end{cases} \tag{22}$$

$$P_{available} = P_{Dn}(n_{Dn}) + \left(P_{En\_PTI}(n_{En}) - P_{En\_PTO}(n_{En}) \right) \tag{23}$$

3.4. Propulsion mode selection

Selection of the optimal propulsion mode is based on the required propulsion power, according to the following criteria:

- Required power estimated by the power estimation,
- Availability of the machinery (shutdown),
- Health state of machinery (slow down / power limits / state of charge),
- Selected mode of operation,
- Optimal specific fuel consumption of the diesel engine, electric motor.

When the above-mentioned variables change, the selected propulsion mode needs to be evaluated by the rule based machinery selection algorithm. Depending on the requested propulsion - and hotel power, available power and propulsion mode, the algorithm can select the optimal mode of operation according to Table 2.

No.	PORT DIESEL D_1	STBD DIESEL D_2	PORT GENERATOR G_1	STBD GENERATOR G_2	BATTERIES B_1	PORT SHAFTMACHINE E_1	STBD SHAFTMACHINE E_2	MODE OF OPERATION	PROPULSION MODE	COMMENT
1			HOTEL					TRANSIT	DIESEL DIRECT	
2				HOTEL				TRANSIT	DIESEL DIRECT	
3					HOTEL			TRANSIT	DIESEL DIRECT	
4					CHARGE	HOTEL	HOTEL	TRANSIT	PTO	Normal charge
5					PEAK SHAVE	HOTEL	HOTEL	TRANSIT	PTO	
6			HOTEL			PTI	PTI	TRANSIT	ELECTRIC	
7				HOTEL		PTI	PTI	TRANSIT	ELECTRIC	
8				HOTEL		PTI	PTI	TRANSIT	ELECTRIC	
9			HOTEL	HOTEL		PTI	PTI	TRANSIT	ELECTRIC	
10			HOTEL		CHARGE	PTO	PTO	TRANSIT	PTO	Normal charge
11				HOTEL	CHARGE	PTO	PTO	TRANSIT	PTO	Fast charge
12			HOTEL	HOTEL	CHARGE			TRANSIT	DIESEL DIRECT	Fast charge
13			HOTEL		CHARGE	PTO	PTO	TRANSIT	PTO	Ultra fast charge
14			HOTEL	HOTEL		PTI	PTI	TRANSIT	BOOST	
15				HOTEL		PTI	PTI	TRANSIT	BOOST	
16					HOTEL	PTI	PTI	TRANSIT	BOOST	Battery boost
17			HOTEL			PTI	PTI	HARBOUR	BOOST	
18				HOTEL		PTI	PTI	HARBOUR	BOOST	
19					HOTEL	PTI	PTI	HARBOUR	BOOST	Battery boost
20			HOTEL					HARBOUR	DIESEL	
21				HOTEL				HARBOUR	DIESEL	
22					HOTEL			HARBOUR	DIESEL	
23					HOTEL	PTI	PTI	HARBOUR	ELECTRIC	Zero emmision
24			HOTEL			PTI	PTI	HARBOUR	ELECTRIC	Low emmision
25				HOTEL		PTI	PTI	HARBOUR	ELECTRIC	Low emmision
26			HOTEL	HOTEL		PTI	PTI	HARBOUR	ELECTRIC	Low emmision
27			HOTEL			PTO	PTI	TRANSIT	PTO/ ELECTRIC	Crossshaft
28				HOTEL		PTI	PTO	TRANSIT	ELECTRIC / PTO	Crossshaft

Legend:
- ☐ = MACHINERY OFF
- ▨ = MACHINERY ACTIVE
- HOTEL = HOTEL LOAD
- CHARGE = CHARGE BATTERIES

Table 2 Propulsion mode selection table

If machinery healthy states change, it could be that the selected propulsion mode cannot be maintained or the actual power is reduced (ΔP is far positive in Figure 13). In this case, a kinaesthetic force as function of the lever position can be applied. The kinaesthetic force will reduce PRL lever position to a point that matches the actual power given by the propulsion devices. This is supported by a visual and acoustic warning, to signal the master about the abnormality.

3.5. *Propulsion mode transitions*

During mode transition, the machinery is set to different operating states (like started, stopped, synchronized and ready for torque transfer). Depending on the propulsion mode, thrust is kept steady during the mode transition. The mode transition can fail due to machinery health problems. In this case, the mode transition is aborted and the current propulsion mode is maintained.

A mode transition is initiated by the master operating the PRL. The haptic control algorithm informs the master via haptic patterns (bi-directional interaction). Figure 14 shows on the left side an example of the mode transition (from A to B). The master increases the power request via the PRL until it reaches a detent. By pushing further, a (stiff) spring force (kinaesthetic) feedback is added in order to inform the master about the limitations of the current propulsion mode. By keeping the PRL for predefined time in this area, the mode transition is initiated. During the mode transition, increased friction and the vibro-tactile effect is executed as a haptic pattern, until the mode transition is successfully completed. Power operating limits are updated accordingly.

In case the mode transition fails, the amplitude and frequency of the vibro-tactile effect is increased significantly in order to inform the master about the failed mode transition (Figure 14 right). A mode transition failure is also indicated by a visual and acoustic warning.
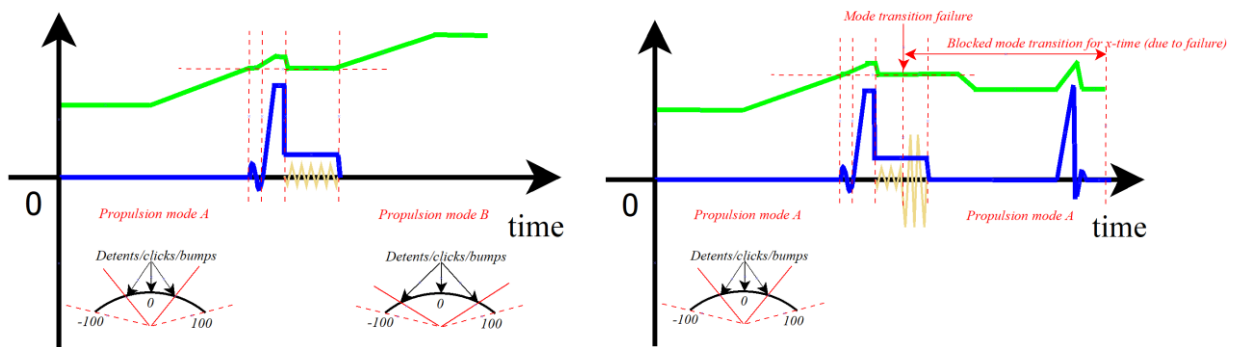
Figure 14: Haptic pattern during mode transitions

3.6. Crash-stopping

During crash stopping it is important to generate as much negative thrust as possible to reduce the head reach of the vessel. For a vessel with CPPs, crash-stopping is achieved by reversing the propeller pitch angle while maintaining the rotational direction of the propeller. As this can be achieved in a relatively short time the incoming speed of the water isn't reduced when the propeller pitch is decreased towards zero. When a crash stop is initiated at high ship speed this could cause wind-milling of the propeller. In this case the propeller gives a negative torque, i.e. drives the shaft-line, increasing the propeller speed with a potential risk of over-speeding the diesel engine. Wind-milling is avoided by temporary stopping the reduction of the propeller pitch and / or speed towards zero, until the incoming water speed at the propeller is reduced.

For a hybrid propulsion system the PTO shaft-generator can be used as a dynamic shaft brake absorbing the negative torque energy from the propeller. This can result in a lower risk of overspeed and faster pitch reversing, resulting in a shorter head reach of the vessel when a crash stop is executed.

In machinery control systems wind-milling of the propeller can be detected based on the difference between the actual and demanded shaft-speed, PRL position, ship-speed and diesel-engine fuel demand. In case of wind-milling, the pitch rate to astern rate will be reduced automatically. This reduction can be used as input for kinaesthetic force feedback (dynamic friction) in the PRL as shown in Figure 15. In this way the master is made aware that the actual pitch angle is lagging on the requested demand. If the negative torque sufficiently reduced, kinaesthetic force level reduces and the propeller pitch can be reversed by moving the PRL in the astern direction (through zero).
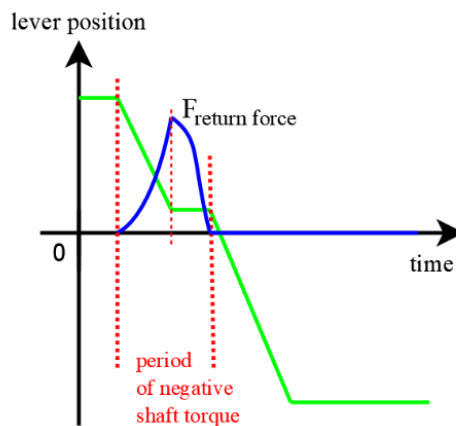
Figure 15: Example of kinaesthetic force during crash stop

4. Conclusion

The step towards automation in recent decades involves optimization and integration of systems. At the same time, it is known that over-automation has led to increasing complexity and fails to account for human factors. This complexity and many degrees of freedom to operate the vessel causes negative effects for masters. The excessive visual overload leads to a loss of situational awareness that in turn harms performance and safety.

With bi-directional PRL lever haptics, the master becomes able to use the neuro sensing system of touch and feel. This allows the masters' visual sensing system to focus on observing the vessels' motions. The reduction of workload and addition of human sensing drastically increases the masters' situational awareness and consequently increases the safety of manoeuvring. Although the accident onboard of the USN destroyer John McCain was, besides other aspects like tiredness, a presence of an intuitive steering wheel with haptic force feedback could have led to avoidance of the accident. The PRL lever haptics, to operate the main propulsion hybrid power ferry, allows the master to cope with the increased complexity of the addition of electric shaft-machines and batteries. The master intuitively sets the PRL position to achieve the vessels' intended motions. By setting the mode of operation (harbour or transit), the PRL demands the required power. A rule-based PMS, combined with mode selection and bi-directional interaction via haptic patterns, reduces the complexity for the master. The combination selects the most fuel-efficient and feasible machinery configuration and transmits start/stop signals to the machinery. The master receives information on the progress of the transition and is informed by the lever haptics once the requested power has become available. Besides the transition to different propulsion modes, haptic patterns allow to improve the situational awareness during crash-stopping.

It is evident that under all circumstances the master must be certain that the demanded thrusts are achieved, at each propulsion mode. The obvious solution is to apply the PRL lever haptics to reduce complexity and ensure safety by the addition of carefully selected intuitive haptic patterns.

5. Nomenclature

α_1, α_2	PORT / STBD propeller pitch [-]
α_n	Propeller pitch [-]
δ	Propulsion mode [-]
ε	Apparent wind angle [°]
$\varphi_{t1}, \varphi_{s1}, \varphi_{a1}, \varphi_{PRL}$	Position measurement transmitter, -sensor, -actuator and -PRL lever [°]
$\varphi_{thrusters}$	Position of the transverse thruster lever [°]
$\varphi_{PORT}, \varphi_{STBD}$	Position of the PORT / STBD power reversing lever [°] of maximum ship speed
φ_n	Position of the power reversing lever [°]
ρ_{air}	Density of air [kg/m³]
u_{ground}	Speed over ground [m/s]
u_{ship}	Ship speed [m/s]
u_{water}	Speed through water [m/s]
u_{wind}	Apparent wind speed [m/s]
A_F	Frontal projected area [-]
C_t	Thrust coefficient [-]
CX_{AF}	Wind coefficient in surge direction [-]
D_n	Diesel engine number [-]
E	Angle of attack relatively to the bow of the vessel [°]
E_n	Shaft machine number [-]
$J_{t1}, J_{s1}, J_{a1}, J_{gPRL}$	Inertia transmitter, -sensor, -actuator and - PRL lever []
K_{cpp}	Propeller torque coefficient as function of pitch angle [-]
K_{cpp0}	Propeller torque coefficient at zero pitch [-]
K_{power}	Power factor [$W \cdot N^{-1}$]
K_{safety}	Safety factor to increase the thrust demand force [-]
n	Propeller / device number [-]
N_1, N_2	PORT / STBD propeller speed [n-1]
N_{D1}, N_{D2}	PORT / STBD diesel engine speed [n-1]
N'_{D1}, N'_{D2}	PORT / STBD gearbox output shaft speed [n-1]
N_{Dn}	Diesel engine speed [n-1]
N_n	Propeller speed [sec^{-1}]
P	Pitch polynomial [-]
P_1, P_2	PORT / STBD actual propeller power [W]
$P_{available}$	Available power for machinery [W]
P_{aux}	Total auxiliary load of the vessel [W]
P_{B1}, P_{B2}	PORT / STBD battery power [W]
P_{D1}, P_{D2}	PORT / STBD diesel engine power [W]
P_{Dn}	Diesel engine power [W]
P_{Dn_MCR}	Maximum continues rated diesel engine power [W]

$P_{Dn\_SLOWDOWN}$	Maximum continues rated diesel engine power during a slowdown situation [W]
P_{E1}, P_{E2}	PORT / STBD shaft machine power [W]
P_{En}	Shaft machine power [W]
P_{En_PTI}	Actual available shaft machine power in PTI mode [W]
$P_{En\_PTI\_PWR\_LIMIT}$	Maximum allowed shaft machine power in PTI mode [W]
P_{En_PTO}	Actual available shaft machine power in PTO mode [W]
$P_{En\_PTO\_PWR\_LIMIT}$	Maximum allowed shaft machine power in PTO mode [W]
P_{G1}, P_{G2}	PORT / STBD auxiliary generator power [W]
P_{Gn}	Auxiliary generator power [W]
P_{hotel}	Total hotel load of the vessel [W]
P_{LOAD_LIMIT}	Load limit set by the chief engineer per a propulsion device [%]
$P_{n\_required}$	Required power for harbour mode [W]
P_n	Actual propeller power [W]
P_{PTI_MAX}	Maximum shaft machine PTI (motoring) power [W]
P_{MAX_THR}	Maximum shaft machine PTI (motoring) power [W]
P_{PTI_MAX}	Maximum shaft machine PTI (motoring) power [W]
$P_{thrusters}$	Transverse thruster power for harbour mode [W]
$P_{thrusters\_max}$	Maximum transverse thruster power [W]
$P_{total\_required}$	Total vessel power requirement [W]
Q_1, Q_2	PORT / STBD propeller torque [Nm]
Q_n	Propeller torque [Nm]
$Q_{n\_required}$	Required torque for harbour mode [Nm]
Q_{D1}, Q_{D2}	PORT / STBD diesel engine torque [Nm]
$Q`_{D1}, Q`_{D2}$	PORT / STBD gearbox output shaft torque [Nm]
Q_{Dn}	Torque produced by diesel engine [Nm]
Q_{E1}, Q_{E2}	PORT / STBD shaft machine torque [Nm]
Q_{En}	Shaft machine torque [Nm]
$Q_{En\_MAX\_TORQUE}$	Maximum shaft machine torque [Nm]
$Q_{t1}, Q, Q_{a1}, Q_{gPRL}$	Torque transmitter, -sensor, -actuator and PRL lever [Nm]
R	Pitch force polynomial [-]
R_{total}	Total vessel resistances [N]
T_1, T_2	PORT / STBD propeller thrust [N]
T_{MAX}	Maximum thrust of propellers [N]
T_n	Propeller thrust [N]
$T_{n_{required}}$	Required thrust force for harbour manoeuvring [N]
$T_{thrusters\_max}$	Maximum transverse thruster thrust force for harbour manoeuvring [N]
$T_{thrusters\_required}$	Required transverse thruster thrust force for harbour manoeuvring [N]
T_{x_wind}	Wind force in surge (x) direction [N]
T_{y_wind}	Wind force in sway (y) direction [N]

6. Glossary of terms

AC	Alternating current
CPP	Controllable Pitch Propeller
DC	Direct current
ETA	Expected Time of Arrival
FPP	Fixed Pitch Propeller
PORT	Port side
PTO	Power Take Off
PTI	Power Take In
PMS	Power Management System
PRL	Power Reversing Lever
STBD	Starboard side
SOC	State of charge [%]

7. References

1. Armstrong-Hélouvry, B., Dupont, P., & De Wit, C. C. (1994). A survey of models, analysis tools and compensation methods for the control of machines with friction. Automatica, 30(7), 1083-1138.
2. Asif, A., Heuten, W., & Boll, S. (2010, October). Exploring distance encodings with a tactile display to convey turn by turn information in automobiles. In Proceedings of the 6th Nordic conference on human-computer interaction: Extending boundaries (pp. 32-41).
3. Barrow, A., & Harwin, W. (2016). Design and analysis of a haptic device design for large and fast movements. Machines, 4(1), 8.
4. Bernstein, N. L., Lawrence, D. A., & Pao, L. Y. (2005, March). Friction modeling and compensation for haptic interfaces. In First Joint Eurohaptics Conference and Symposium on Haptic Interfaces for Virtual Environment and Teleoperator Systems. World Haptics Conference (pp. 290-295). IEEE.
5. Boff, K. R., Kaufman, L., & Thomas, J. P. (Eds.). (1986). Handbook of perception and human performance.
6. Bossert, V. et al. (2017), More efficient diesel-electric power-plant for dredgers, Dredging Summit & Expo '17 Proceedings.
7. Chawda, V., Celik, O., & O'Malley, M. K. (2018). Evaluation of velocity estimation methods based on their effect on haptic device performance. IEEE/ASME Transactions on Mechatronics, 23(2), 604-613.
8. Colgate, J. E., & Brown, J. M. (1994, May). Factors affecting the z-width of a haptic display. In Proceedings of the 1994 IEEE International Conference on Robotics and Automation (pp. 3205-3210). IEEE.
9. Einsiedler. M. (2017). Hybrid Energy and Propulsion System for Vessels in Timetable Operation, Technology and Science for the Ships of the Future.
10. El Saddik, A., Orozco, M., Eid, M., & Cha, J. (2011). Haptics technologies: bringing touch to multimedia. Springer Science & Business Media.
11. Ghaffari, T. K., & Kövecses, J. (2013, April). A high-performance velocity estimator for haptic applications. In 2013 World Haptics Conference (WHC) (pp. 127-132). IEEE.
12. Gosselin, F., Ferlay, F., & Janot, A. (2016, June). Development of a new backdrivable actuator for haptic interfaces and collaborative robots. In Actuators (Vol. 5, No. 2, p. 17). Multidisciplinary Digital Publishing Institute.
13. Grimmelius, H., de Vos, P., Krijgsman, M., & van Deursen, E. (2011, May). Control of hybrid ship drive systems. In 10th International conference on computer and IT applications in the maritime industries (pp. 1-15).
14. Grunwald, M. (Ed.). (2008). Human haptic perception: Basics and applications. Springer Science & Business Media.
15. Haruhisa, K. (2015). Robot Hands and Multi-fingered Haptic Interfaces: Fundamentals and Applications. World Scientific.
16. Karnopp, D. (1985). Computer simulation of stick-slip friction in mechanical dynamic systems.
17. Kilchenman, R., & Goldfarb, M. (2001, May). Force saturation, system bandwidth, information transfer, and surface quality in haptic interfaces. In Proceedings 2001 ICRA. IEEE International Conference on Robotics and Automation (Cat. No. 01CH37164) (Vol. 2, pp. 1382-1387). IEEE.
18. Kosuge, K., Fujisawa, Y., & Fukuda, T. (1992, July). Control of mechanical system with man-machine interaction. In Proceedings of the IEEE/RSJ international conference on intelligent robots and systems (Vol. 1, pp. 87-92). IEEE.
19. Lawrence, D. A. (1993). Stability and transparency in bilateral teleoperation. IEEE transactions on robotics and automation, 9(5), 624-637.
20. Minsky, M. D. R. (1995). Computational haptics: the sandpaper system for synthesizing texture for a force-feedback display (Doctoral dissertation, Massachusetts Institute of Technology).
21. National Transportation Safety Board. (2019). Collision between US Navy Destroyer John S McCain and Tanker Alnic MC, Singapore Strait, 5 Miles Northeast of Horsburgh Lighthouse, August 21, 2017. Marine Accident Report NTSB/MAR-19/01.
22. Pacchierotti, C. (2015). Cutaneous haptic feedback in robotic teleoperation. Springer International Publishing.
23. Qin, H., Song, A., Liu, Y., Jiang, G., & Zhou, B. (2015). Design and calibration of a new 6 DOF haptic device. Sensors, 15(12), 31293-31313.
24. Qin, H.; Song, A.; Liu, Y.; Jiang, G.; Zhou, B. Design and calibration of a new 6 DOF haptic device. Sensors 2015, 15, 31293–31313
25. Rauer, E. (2019). Methodology to Analyse Handling Qualities Under Force Gradient Transitions of an Active Sidestick. Aerotecnica Missili & Spazio, 98(3), 231-242.

26. Rovers, A. F., Steinbuch, M., & Lammerts, I. M. M. (2003). Design of a robust master-slave controller for surgery applications with haptic feedback. Technische Universiteit Eindhoven.

27. Shimoga, K. B. (1992). Finger force and touch feedback issues in dextrous telemanipulation. In Proc. NASA-CIRSSE Int. Conf. Intelligent Robotic Systems for Space Exploration.

28. Tsuji, T., Goto, K., Moritani, M., Kaneko, M., & Morasso, P. (1994, September). Spatial characteristics of human hand impedance in multi-joint arm movements. In Proceedings of IEEE/RSJ International Conference on Intelligent Robots and Systems (IROS'94) (Vol. 1, pp. 423-430). IEEE.

29. Ueberle, M. W. (2006). Design, control, and evaluation of a family of kinesthetic haptic interfaces (Doctoral dissertation, Technische Universität München).

30. Van der Linde, R. Q., Lammertse, P., Frederiksen, E., & Ruiter, B. (2002, July). The Haptic Master, a new high-performance haptic interface. In Proc. Eurohaptics (pp. 1-5).

31. Weber, B., Schätzle, S., Hulin, T., Preusche, C., & Deml, B. (2011, June). Evaluation of a vibrotactile feedback device for spatial guidance. In 2011 IEEE World Haptics Conference (pp. 349-354). IEEE.

32. Werner Blendermann (1994), Parameter identification of wind loads on ships. In Journal of Wind Engineering and Industrial Aerodynamics Volume 51, Issue 3, May 1994, Pages 339-351.